Diffusion Behavior of Cumulative He Doped in Cu/W Multilayer Nanofilms at Room Temperature *

Ling Wang(王玲)[1,3], Wang Liu(刘望)[1], Yue Li(李悦)[2], Yun-Long Shi(石云龙)[2], Yuan-Xia Lao(劳远侠)[1], Xiao-Bo Lu(卢晓波)[2], Ai-Hong Deng(邓爱红)[1,2**], Yuan Wang(汪渊)[1**]

[1]*Key Laboratory for Radiation Physics and Technology (Ministry of Education), Institute of Nuclear Science and Technology, Sichuan University, Chengdu 610064*

[2]*College of Physical Science and Technology, Sichuan University, Chengdu 610064*

[3]*School of Nuclear Engineering and Geophysics, East China University of Technology, Nanchang 330013*

(Received 13 October 2015)

Cu/W multilayer nanofilms are prepared in pure Ar and He/Ar mixing atmosphere by the rf magnetron sputtering method. The cross-sectional morphology and the defect distribution of the Cu/W multilayer nanofilms are characterized by scanning electron microscopy and Doppler broadening positron annihilation spectroscopy. The results show that plenty of point defects can be produced by introducing He during the growth of the multilayer nanofilms. With the increasing natural storage time, He located in the near surface of the Cu/W multilayer nanofilm at room temperature could be released gradually and induce the segregation of He-related defects due to the diffusion of He and defects. However, more He in the deep region spread along the interface of the Cu/W multilayer nanofilm. Meanwhile, the layer interfaces can still maintain their stability.

PACS: 68.65.Ac, 68.37.−d, 68.35.Fx DOI: 10.1088/0256-307X/33/6/066801

The advantage of utilizing a multilayer film in the study of its irradiation tolerance property is the existence of layer interfaces, which can act as the sink positions of the point defects migrating and annihilating.[1−4] The immiscible metal layer interface of multilayer nanofilms can effectively reduce the formation of voids, clusters and He bubbles.[5−7] Recent studies have shown that, compared with conventional single-phase bulk metals, the interfaces in composite materials can act as sinks for irradiation-induced defects, promote recombination of point defects and result in enhanced irradiation tolerance. For instance, Cu/W multilayer films were morphologically stable and no obvious amorphous regions were formed under 50 keV He ions with fluence from $7 \times 10^{20}/\mathrm{m}^2$ to $6 \times 10^{21}/\mathrm{m}^2$ irradiation.[1] He bubbles were observed to align the layer interfaces of the Cu/Nb multilayers irradiated by 33 keV He ions with a dose of $6 \times 10^{20}/\mathrm{m}^2$.[2] Moreover, the annealed Cu/Nb multilayer thin film with 4 nm layer thickness showed a higher morphological stability of the nanolayered structure than the Cu reference sample.[6]

However, the efforts of most works have only focused on obtaining the threshold values of irradiation resistance of the multilayer films by single irradiation (such as ion implantation) with different irradiation energies and/or doses.[1,4,8] In fact, He with certain energy implants into materials and produces displacement damage along with the collision trajectory,[9,10] then the following step is a long-term diffusion damage period of He. For example, in a plasma facing material (PFM), such as tungsten, the accumulation damage of He-vacancy complexes or He bubbles can be formed by this kind of long-term diffusion and coalescence of He.[11] The evolution of He-related defects can change the microstructure of the PFMs, and even cause serious degradation of macroscopic properties of the materials, such as swelling and cracking.[12] However, a fundamental understanding of the impacts of the long-term diffusion behavior of cumulative He and the stability of layer interfaces on the service properties and lifetime of the multilayer nanofilms remain largely unknown.

In this Letter, we present an effective method for introducing He into as-grown nanofilms by magnetron sputtering under He/Ar mixed atmosphere. Unlike the traditional method of He implantation, plenty of He atoms could be continuously and homogeneously introduced into specimens with no displacement damage.[13,14] The diffusion behavior of cumulative He in Cu/W multilayer nanofilms at room temperature is studied by scanning electron microscopy (SEM) and Doppler broadening positron annihilation spectroscopy (DB-PAS). The stability of layer interfaces of Cu/W multilayer nanofilms is also investigated.

The Cu/W multilayer nanofilms were deposited on single crystal Si (100) substrates. A W plate (99.95%, purity) and a Cu plate (99.995%, purity) were used as the targets mounted on the water-cooled cathodes during deposition. The base pressure of the sputtering system was 1.0×10^{-4} Pa. The substrates were

*Supported by the National Natural Science Foundation of China under Grant Nos 11275132, 51171124 and 11505121, the International Science and Technology Cooperation Program of China under Grant No 2014DFR50710, and the Scientific and Technical Supporting Programs Funded by the Science and Technology Department of Sichuan Province under Grant No 2014GZ0004.

**Corresponding author. Email: wyuan@scu.edu.cn; ahdeng@scu.edu.cn

© 2016 Chinese Physical Society and IOP Publishing Ltd

cleaned ultrasonically with alcohol and acetone in advance, and then were cleaned again by applying an rf power of 100 W under an Ar gas pressure of 2.0 Pa (purity of 99.999%) for at least 15 min prior to film deposition. Before W and Cu layers were deposited, the W target and the Cu target were pre-sputtered for 15 min by Ar ions at the power of 80 W to remove effectively the target surface impurity.

The Cu/W multilayer nanofilms with a modulation period of 25 nm were performed at an rf power of 30 W. The working pressure was controlled at 0.9 Pa by a constant Ar/He mixing gas flow. The substrates were rotated to avoid concentration gradients of the films. The deposition was performed at room temperature, and the maximum elevated temperature of the substrate holder was less than 100℃ during deposition. The samples a2 and a3 were deposited at the same time within He/Ar mixed atmosphere, while the sample a1 was prepared under pure Ar atmosphere. To investigate the diffusion behavior of cumulative He at room temperature, the sample a3 was placed in a vacuumed jar for five months after deposition.

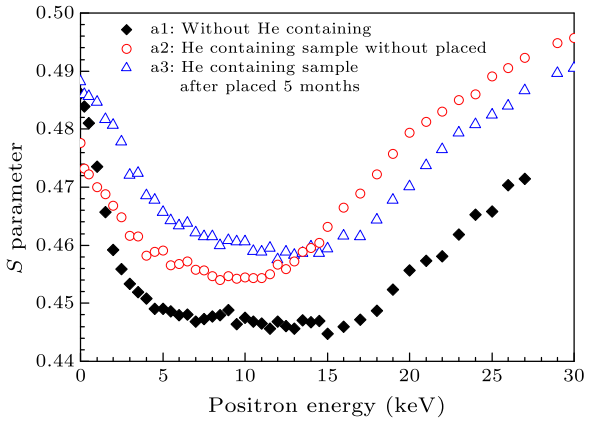

Fig. 1. The S parameter curves of DB-PAS for the Cu/W multilayer nanofilms a1, a2 and a3.

The cross-sectional morphologies of the samples were determined by a field emission scanning electron microscope (FESEM, SHIMADZU S-4800). The measurements of DB-PAS were carried out at room temperature by using an energy-variable slow positron beam. In this measurement system, the β^+ decay of a ^{22}Na radioactive source was used to obtain positrons, which was slowed down and transmitted through the vacuum pipe of a magnetically controlled system. The variable mono-energetic positron beams from 0.1 to 30 keV were used to measure the depth profile of defects in Cu/W multilayer nanofilms. A HpGe detector with an energy resolution of approximately 1 keV was mounted perpendicular to the beam direction, and was used to measure the Doppler energy broadening of the 511 keV$\pm\Delta E$ gamma rays which were released by positron annihilation. Here ΔE was the Doppler shift of the annihilation photon and was proportional to the kinetic momentum of the annihilation electron in the direction of propagation of the 511 keV photon.[9,12,15,16] For each positron incident energy, spectrum with total counts of 1.0×10^6 was collected for the 511 keV annihilation peak.

The DB-PAS data of the slow positron beam are shown in Fig. 1. The S–E curves of three samples follow a similar pattern as shown in Fig. 1. A platform region (the middle section) and two dramatic changing regions (the surface section and the near substrate section) can be found in these curves.

Positrons in the energy range of 0–5 keV probe primarily the surface information of samples and this region is denoted as the surface section. The positrons with low incident energy usually have negative power function in the metals of Cu and W and can easily be scattered back to the sample surface and then interacted with the surface of the specimen.[15] These positrons scattered back to the surface would be trapped by the image potential well or the defects on the surface.[15–18] The impurity may be generated due to the surface oxidation in the process of the storage, which also increases the capture probability of the positrons.[18] Therefore, the higher S values can be found at the beginning of the S–W curves.

The probability of positrons back diffusion to the surface reduces and most positrons mainly stay in the middle section of Cu/W multilayer nanofilm with the increasing positron beam energy. The S values in this section, which are located mainly in the bulk region of the multilayer nanofilm, present some relatively smooth and flat platform as shown in Fig. 1. It is indicated that the distribution of defects is relatively homogeneous in the middle section. However, it can be seen that the lengths of three platforms are not similar in Fig. 1. The platform length (in the range of 5–16 keV) of the sample a1 is longest compared with those of both samples a2 and a3. This indicates that the homogeneous region of samples becomes narrower due to the introduction of He. In addition, the platform length of the sample a3 (range of 5–15 keV) is longer than that of the sample a2 (range of 5–12.5 keV). It is implied that the homogeneous region of the sample a3 is wider than that of the sample a2. This can be attributed to the diffusion of defects and He to induce the distribution of the defects to become relatively homogeneous in the sample a3 during the long-term storage.

With the incident energy increasing further, the positrons penetrate into the near substrate section. The S values of the curves begin to increase significantly. This can be attributed to the unstable microstructure of multilayer nanofilms at their initial growth stage. In addition, plenty of defects generated by the lattice mismatch of the multilayer nanofilm and the Si substrate may also result in the increase of the S parameter.

The cross-sectional morphologies of the three samples are shown in Fig. 2. It can be seen that numerous He bubbles distribute homogeneously in the sample a2 compared with the sample a1 (Figs. 2(a) and 2(b)). It is indicated that plenty of point defects are generated in the Cu/W multilayer nanofilms by introducing He. He could be easily trapped by point defects, and then formed He-vacancy complexes or He bubbles.[12] Meanwhile, the S values of samples a2 and a3 are greater than that of the sample a1 as shown in Fig. 1. It is also implied that the defect concentrations or sizes of samples a2 and a3 are higher than those of the sample a1. The SEM results are in agreement with the S–E curves. However, the distribution of He bubbles becomes inhomogeneous after placed for five months compared with the sample a2 (Figs. 2(b) and 2(c)). Due to the fact that samples a2 and a3 were deposited at the same time with the same preparation process, they should have the consistent initial condition. Our previous work has also obtained that He average concentrations of samples a2 and a3 were all about 5.20×10^{17} at./cm^2[19] measured by enhanced proton backscattering spectrometry (EPBS).[20] Thus at the beginning both samples a2 and a3 have the same He average concentration. With the increasing natural storage time, He in the sample a3 would be released gradually due to He diffusion,[21–23] and some of the deformed lattices around He bubbles were recovered accordingly.[23] Therefore, the average concentration of the defects probably decreases after being placed for five months. From Fig. 1, it can be seen that the S values in the near substrate section of the sample a3 are exactly lower than that of the sample a2. It implies that the defect concentration in the near substrate section of the sample a3 reduces.

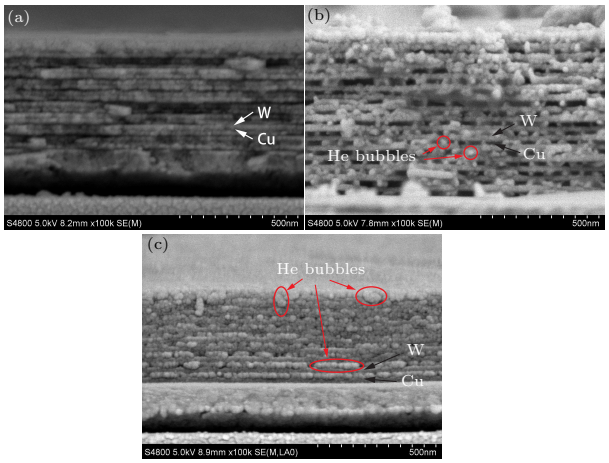

Fig. 2. The cross-sectional morphologies of SEM for the three samples. (a) Sample a1 without He containing, (b) sample a2 with He doped, and (c) sample a3 placed after five months.

However, the S values of the sample a3 are greater than that of the sample a2 in the surface and middle section in Fig. 1. The reason may be that some of the released He could be trapped by the defects and redeposit on the surface of the metal to form He-related defects.[23,24] Accordingly, some larger He bubbles are found in the surface section of the sample a3 as shown in Fig. 2(c) due to the segregation of He related defects. In addition, He bubbles spreading into flaky state can be observed to diffuse continuously along the layer interfaces in the middle section of Cu/W multilayer nanofilm (Fig. 2(c)). This is due to the fact that some interstitial He atoms may also migrate to the deep region of the nanofilm and can easily be trapped by the defects to form more He bubbles due to its insolubility in metallic materials.[12] Previous studies have found that He bubbles aggregated more easily along the layer interfaces of multilayer films.[2,3] It is concluded that the diffusion of He induces the increase of the size or the number of the defects in the surface and middle section of the sample. It is noteworthy that the layer interfaces of the sample a3 are still stable and no cracking or peeling phenomena can be observed from Fig. 2.

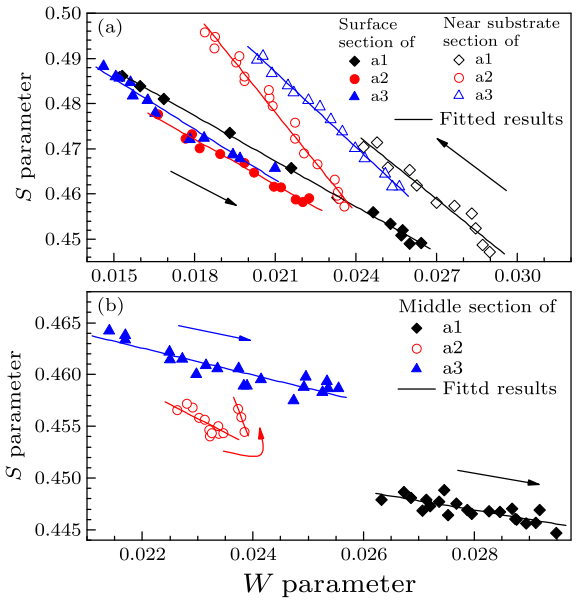

Fig. 3. The S–W curves of Cu/W multilayer nanofilms, and the solid lines are the fitted results. The arrows indicate the direction of increasing positron incident energy. (a) The S–W curves of the surface section (0–5 keV) and the near the substrate section (16–27 keV for a1, 12.5–30 keV for a2 and 15–30 keV for a3, respectively). (b) The S–W curves of the middle section (5–16 keV for a1, 5–12.5 keV for a2 and 5–15 keV for a3, respectively).

The S–W plot of DB-PAS is typically used to identify the number of defect types. When only one type of defect exists in the sample, the S–W plot can be fitted as a linear function due to the fact that every kind of positron annihilation site is characterized by a typical (S, W) couple.[8,9] As shown in Fig. 3, the $S(E)$ and $W(E)$ data of three samples are plotted as trajectories in the S–W plane, by using the incident energy as a running parameter. The arrows denote

the direction of the incident energy increasing. The different trapping section is characterized by (S, W) coordinates.

As seen from Fig. 3(a), the S–W plots in the surface section of three samples follow the linear relationship. It implies that only one type of defect exists in the surface section of each sample. Likewise, only one type of defect is detected existing in the near substrate section of each sample (Fig. 3(a)). In Fig. 3(b), the data of the middle section of samples a1 and a3 still follow a similar linear relationship, thus also probably only one type of defect prevails in this section of samples a1 and a3. However, the sample a2 has a different trend in this section, which presents a curved trajectory for the S–W plot.

The middle section, which is relatively far from the surface and substrate, can hardly be affected by the defects in the surface or the unstable microstructure near the substrates of samples. Therefore, the distribution of the defects in the middle section of the sample a1 is relatively homogeneous (Fig. 3(a)). However, He-related defects would be formed in the Cu/W multilayer films by introducing He. The SEM morphology in Fig. 2(b) also exhibits that numerous He bubbles distributed in the sample a2. Thus more than one type of defect is distributed in the middle section of the sample a2. However, with the increasing natural storage time, probably only one type of defect can be found in the middle section of the sample a3 as shown in Fig. 3(b). This result shows that the diffusion of He and defects would induce the defect type to be accordant gradually in the middle section of the sample a3.

In summary, plenty of point defects can be produced during the growth of Cu/W multilayer nanofilms by the introduction of He, which has an impact on the homogeneity and type of defects in the nanofilms. The experimental results indicate that the diffusion of He and defects at room temperature results in the increase of the defect size or number in the surface and middle sections of nanofilms. Moreover, with the increasing natural storage time, He atoms located in the near surface of Cu/W multilayer nanofilms could be released gradually and induce the segregation of He-related defects due to the diffusion of He and defects. More He atoms in the deep region spread along the interface of Cu/W multilayer nanofilm, and the defect type generally tends to be uniform. Meanwhile, the layer interfaces can still maintain their stability.

References

[1] Gao Y, Yang T F, Xue J M, Yan S, Zhou S Q, Wang Y G, Chu P K and Zhang Y W 2011 *J. Nucl. Mater.* **413** 11
[2] Zhang X, Li N, Anderoglu O, Wang H, Swadener J G, Hochbauer T, Misra A and Hoagland R G 2007 *Nucl. Instrum. Methods Phys. Res. Sect.* B **261** 1129
[3] Li N, Fu E G, Wang H, Carter J J, Shao L, Maloy A, Misra A and Zhang X 2009 *J. Nucl. Mater.* **389** 233
[4] Demkowicz M J, Misra A and Caro A 2012 *Curr. Opin. Solid State Mater. Sci.* **16** 101
[5] Shen T D, Feng S H, Tang M, Valdez J A and Wang Y Q 2007 *Appl. Phys. Lett.* **90** 263115
[6] Hchbauer T, Misra A, Hattar K and Hoagland R G 2005 *J. Appl. Phys.* **98** 123516
[7] Wang Y C, Misra A and Hoagland R G 2006 *Scr. Mater.* **54** 1593
[8] Lhuillier P E, Belhabib T, Desgardin P, Courtois B, Sauvage T, Barthe M F, Thomann A L, Brault P and Tessier Y 2011 *J. Nucl. Mater.* **416** 13
[9] Cao Q S, Jua X, Guo L P and Wang W B 2014 *Fusion Eng. Des. Design* **89** 1011
[10] Glenn F K 1999 *Radiation Detection and Measurement* (New York: Chichester) chap 2 p 30
[11] Bhuyan M, Mohanty S R and Rao C V S 2013 *Appl. Surf. Sci.* **264** 674
[12] Li Y, Deng A H, Zhou Y L, Zhou B, Hou Q, Shi L Q, Qin X B and Wang B Y 2012 *Chin. Phys. Lett.* **29** 047801
[13] Shi L Q, Liu C Z, Xu S L and Zhou Z Y 2005 *Thin Solid Films* **479** 52
[14] Song Y M, Luo X G, Long X G, An Z, Liu N, Pang H C, Wu X C, Yang B F and Zheng S X 2008 *Chin. Sci. Bull.* **53** 469
[15] Wang S J, Chen Z Q, Wang B, Wu Y C, Fang P F and Zhang Y X 2008 *Applied Positron Spectroscopy* (Hubei: Hubei Science and Technology Press) chap 1 p 40 (in Chinese)
[16] Chen Z Q, Maekawa M, Kawasuso A, Sakai S and Naramoto H 2006 *J. Appl. Phys.* **99** 093507
[17] Chen Z Q, Maekawa M, Yamamoto S and Kawasuso A 2004 *Phys. Rev.* B **69** 035210
[18] Peng Y J and Zhao S L 2011 *Minerals Eng.* **24** 1687
[19] Liu W, Wu Q Q, Chen S L, Zhu J J, An Z and Wang Y 2012 *Acta Phys. Sin.* **61** 176802
[20] Duan Y M 2006 *Master Thesis* (Chengdu: Sichuan University) (in Chinese)
[21] Kawakami T, Tokunaga K and Yoshida N 2007 *J. Nucl. Mater.* **367** 457
[22] Ryazanov A, Matsui H and Kazaryan A V 1999 *J. Nucl. Mater.* **271** 356
[23] Zhang B L, Wang J and Hou Q 2013 *J. Nucl. Mater.* **438** 178
[24] Wilson W D, Bisson C L and Baskes M I 1981 *Phys. Rev.* B **24** 5616